

State of the art about dissimilar metal friction stir welding

Aude Simar & Marie-Noëlle Avettand-Fènoël

To cite this article: Aude Simar & Marie-Noëlle Avettand-Fènoël (2016): State of the art about dissimilar metal friction stir welding, Science and Technology of Welding and Joining, DOI: [10.1080/13621718.2016.1251712](https://doi.org/10.1080/13621718.2016.1251712)

To link to this article: <http://dx.doi.org/10.1080/13621718.2016.1251712>



Published online: 16 Nov 2016.



Submit your article to this journal [↗](#)



View related articles [↗](#)



View Crossmark data [↗](#)

State of the art about dissimilar metal friction stir welding

Aude Simar^a and Marie-Noëlle Avettand-Fènoël^b

^aInstitute of Mechanics, Materials and Civil Engineering (iMMC), Université catholique de Louvain (UCL), Louvain-la-Neuve, Belgium;

^bUniversité Lille 1, Unité Matériaux Et Transformations, Villeneuve d'Ascq, France

ABSTRACT

Friction stir welding is a rather recent welding process (patented in 1991 by Thomas et al., 'Improvements to friction welding' UK patent application no. 9125978.8, US Patent 5460317, 1995) that has shown great potential for welding dissimilar materials even of different metallic nature, e.g. Al to steel, Mg to steel, Al to Ti, Mg to Ti, Al to Cu, Al to Mg. This review presents the specific microstructural features and mechanical properties, in particular tensile strength, of such welds. A focus will be on the material flow and welding defects, on the intermetallic compounds, on constitutional liquation, on particularities related to dissimilar lap welding and finally on process modifications to improve dissimilar friction stir weldability.

ARTICLE HISTORY

Received 15 May 2016
Accepted 13 October 2016

KEYWORDS

Friction stir welding;
dissimilar welding;
aluminium; copper;
magnesium; steel; titanium

Introduction

Friction stir welding (FSW) was patented in 1991 by Thomas et al. [1] from The Welding Institute, UK. This joining process was first employed to weld aluminium alloys, such as 2xxx or 7xxx alloys, difficult to join by conventional fusion welding processes [2–5]. Later its use was extended to magnesium, copper, nickel, titanium alloys and even steels [2–4], composites [6], polymers [7], and it is now widely used for dissimilar materials.

FSW (Figure 1) involves the rotation and advancing of a tool [1–5]. This tool is made of a flat or conical shoulder, eventually containing scrolls. The tool ends with a pin that is sometimes tapered and generally made of features, such as threads, flats or flutes. FSW tool characteristics and consequences on similar welds have been reviewed in Shtrikman [8] and Rai et al. [9]. During the process, an axial pressure is also exerted on the tool. When the welding path is linear, the tool can be tilted to favour the closure of the pin hole behind the tool. For butt welding, the tool penetrates at the interface (Figure 1(a)) between the two plates that are rigidly clamped. The heat generated by the friction between the material and the plates as well as the intense plastic deformation around the tool leads to the joining of the two plates. The weld is sealed by the advancing of the tool. The advancing side (AS) is the side where the vectors of the welding speed and the rotational speed are collinear. On the retreating side (RS), the directions of the latter vectors are opposite. The tool offset is here defined as the distance of insertion of the tool in a given plate (Figure 1(a)). This distance inside the

hardest plate is usually smaller than the tool pin radius when one of the plates to assemble is much harder than the other, like in Al to steel welds as will be discussed in the present review.

If the tool does not advance but is directly moved upwards out of the weld seam, the process is called friction stir spot welding (FSSW). The particularities of FSSW will not be further discussed here, and the reader is referred to the recent review by Yang et al. [10]. Figure 1(b) shows another configuration, lap welding, very classically used in FSW and in FSSW, in particular for dissimilar welding.

Distinct zones can be identified in a friction stirred joint [2,3,5] according to the thermo-mechanical histories they have experienced: the heat affected zone (HAZ), the thermo-mechanical affected zone (TMAZ) and the stir zone (SZ). The nugget or SZ corresponds to the volume of material which is directly deformed by the tool pin. In the zones affected by heat (HAZ, TMAZ and SZ), precipitate formation or dissolution (e.g. in Al alloys) and phase transformations (e.g. in steels or titanium alloys) are expected to occur [2,3,5]. The phase transformation, occurring in the base materials due to heating and not specifically related to dissimilar metal welding, will not be further discussed in this review. The reader is thus referred to previous reviews treating these specific microstructure evolutions also observed in similar welds [2,3,5].

The FSW of dissimilar Al or Mg alloys is slowly starting to be a well-established process in the FSW community. The reader interested by the FSW of dissimilar Al or Mg alloys is referred to previous reviews

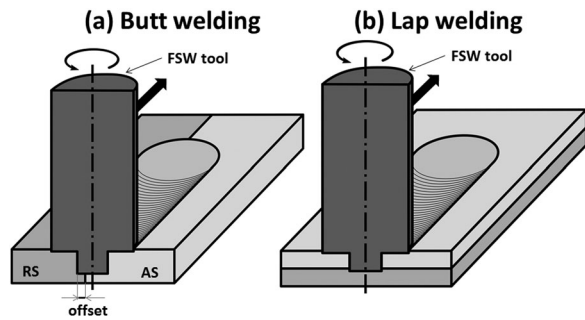


Figure 1. Dissimilar friction stir welding for (a) butt and (b) lap welds. AS, advancing side; RS, retreating side.

[5,11–13]. The present paper will thus focus on dissimilar metal welding, i.e. the welding of metals with distinct chemical compositions. In these welds, specific issues involve the problem of material mixing in the presence of very different high-temperature mechanical properties and constitutive flow laws, the intermetallic compound (IMC) formation and the problem of the constitutional liquation that may lead to local melting. These strongly affect the mechanical properties of the dissimilar welds. The FSW research community has been highly focussed on dissimilar metal welding in the past years as light weighting is a major concern for the transportation (e.g. welding Al to steel) and electrical energy (e.g. welding Cu to Al) industries [14]. Placing the right material at the right place often also imposes to solve the issue of dissimilar welding.

Weld soundness and material mixing in butt welds

Defects related to material flow can be observed in similar welds; however, their appearance is very usual in dissimilar material welds. Indeed, the large difference in flow properties of the base materials at welding temperature perturbs material flow. Such defects may be controlled by the tool geometry, the position of the tool, the material position (softest material on AS or RS) or the welding parameters. Tool wear is also an issue in dissimilar welding particularly when working with very hard materials. As tool wear changes the geometry of its features, it may lead to modification of the material flow and thus decreasing weld performances [15].

Material flow

Two main types of flows are observed in dissimilar metal welds: the vortex-like material flow or the sharp interface, eventually presenting a zigzag shape.

The *vortex-like material flow* looks like fine intercalated or lamellar microstructures with bands rich in one or another base alloy. For example, this was only very locally observed in Al to steel welds [16–21], and more extensively in Al to Ti welds [22–24], Al to Cu welds [25–30] and Al to Mg welds [11,31–34]. Figure 2

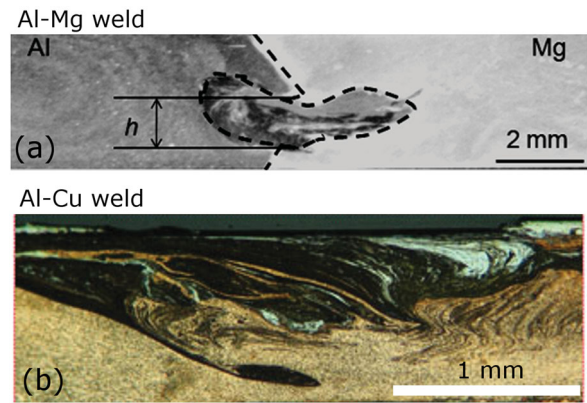


Figure 2. Vortex-like material flow in (a) an Al 6063–Mg AZ31B weld (from Venkateswaran and Reynolds [33]) and (b) an Al 5083–Cu DHP weld (from Galvao et al. [28]).

presents macrographs of vortex-like material flows in Al–Mg and Al–Cu welds. It is expected that the appearance of a vortex-like flow should be favoured when the flow stress at the welding temperature is similar for the two dissimilar metals. These interpenetration zones provide mechanical interlocking and thus improve the properties of the joints, e.g. in Al to Mg dissimilar welds [33]. As the heat input increases, i.e. at high rotational speeds [20,22–24,29,30] and for higher offset of the tool inside the hardest plate [20,24], the vortex-like flow is favoured [20,24,28]. Figure 3 shows the vortex-like flow increase in an Al6Mg to Ti6Al4V dissimilar weld for increasing offset in the titanium plate and for two rotational speeds (see Song et al. [24]).

The *sharp interface* may eventually present a zigzag shape when the tool centre is close to the butted interface, e.g. in Al to Mg welds [34–38] or Al to Cu welds [39]. Sharp interfaces were observed in Al to steel welds [17,20,21,40–43], Al to Ti welds [24,44], Mg to Ti welds [45], Al to Cu welds [28,46–48]. Figure 4 presents macrographs of sharp interface-like material flows in Al–Mg, Al–stainless steel and Al–brass welds. The sharp interface sometimes presents some lamellar structure at the surface due to the shoulder stirring action [17,24,36] (Figure 3) or in the soft material side of the SZ [34,35], where stirring is favoured. This material flow feature is expected to lead to lower weld strength, e.g. in an Al to steel weld [20]. It is generally observed at lower heat input, e.g. for a high-advancing speed in an Al to Cu weld [28], for low-rotational speed and limited tool stirring in the Ti plate in an Al to Ti weld [24] (Figures 3 and 4(c)), for low-rotational speed but high-advancing speed in an Al to Mg weld [33]. This is due to the insufficient heat to allow a good intermixing of both materials since the highest melting point material lacks plasticisation [28]. This does, however, not seem to be observed in Al to Mg welds. Indeed, both materials present similar melting temperatures and expectedly similar plasticisation temperatures. Thus, Somasekharan and Murr [11] and Yan et al. [31] used low-advancing and -rotational speeds

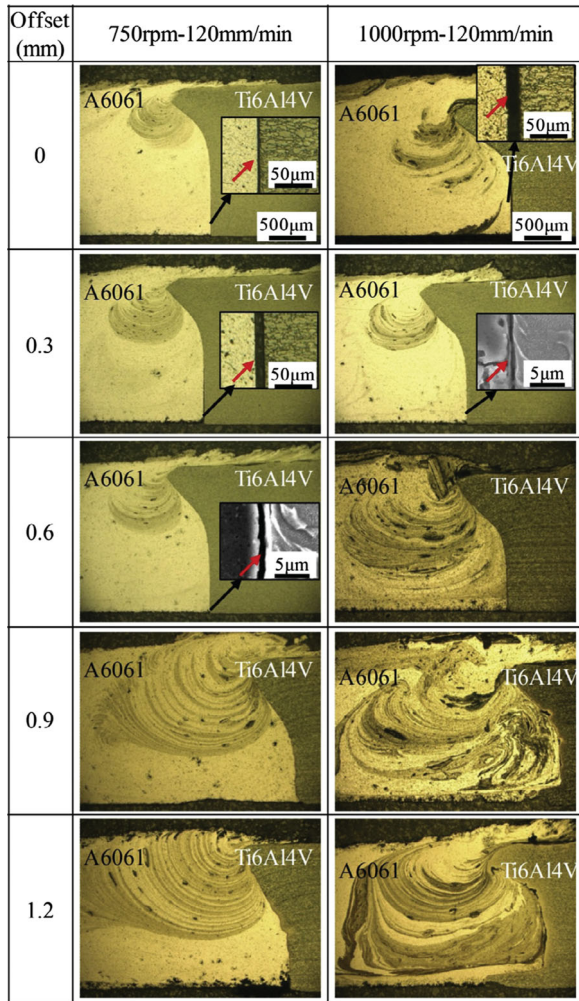


Figure 3. Modification of the material flow in an Al6Mg–Ti6Al4V dissimilar weld for increasing offset in the titanium plate and for two rotational speeds (from Song et al. [24]).

and still obtained vortex-like microstructures in the SZ. In Al to Mg welds, the position of the Al vs. Mg plates seems also to play a role in the transition from one type of feature to the other. Indeed, Fu et al. [34] observed more zigzag-like very sharp features when placing Al on the AS rather than on the RS. Now in Al to Mg welds, the identification of the hardest material is difficult and not clarified in the literature [33,49,50]. For Al to steel welds, Ghosh et al. [40] have compared two designs by placing Al on either AS or RS and found that it had a negligible effect over the general appearance of the interface, presenting a zigzag-like macrostructure in both cases. The joint strength with Al on the AS was not significantly lower than that of the weld performed with the Al placed on the RS.

It is well established that *small or large pieces of the hard material may be observed inside the soft material* in butt welds, e.g. in Al to steel welds [17,19,41,42,51–54] (see Figure 5), in Al to Ti welds [22], in Al to Cu welds [29,55]. A larger tool offset inside the hardest plate placed on the AS of the weld favours the formation of a composite-like structure presenting lots of these hard

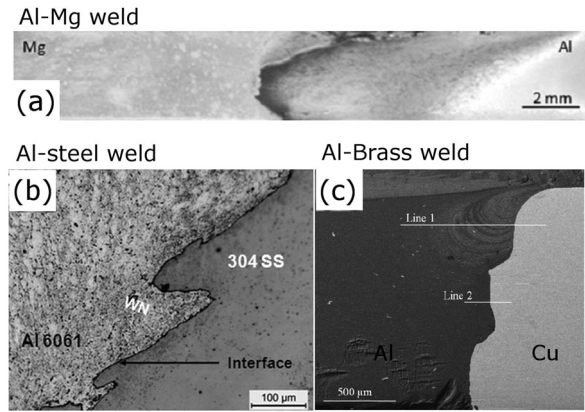


Figure 4. Sharp interface flow in (a) an Al 6063–Mg AZ31B weld (from Venkateswaran and Reynolds [33]), (b) an Al 6061–304 stainless steel weld (from Ghosh et al. [40]) and (c) an Al 1050–brass weld (from Esmaili et al. [46]).

pieces in the softest matrix [51,52,55]. In Al to steel welds, Coelho et al. [17] found such pieces in a larger proportion if the steel is softer, i.e. in HC26OLA steel (BM tensile strength of 397 MPa) compared to a DP steel (BM tensile strength of 625 MPa). Early fracture may be favoured by the presence of such pieces as the fracture path follows them [17,51,52] (see Figure 5(a)). Micro-cracks may be found after welding at the interface of the pieces and the soft material nugget zone [46,51] (see Figure 5(b)). Such micro-cracks are the consequence of the formation of IMCs at that interface, see the section ‘Formation of intermetallic compounds’, and are expected to form during the cooling stage due to the low ductility of these compounds.

Parameters to avoid tunnel defects

The tool geometry and features may impact the formation of defects. Dehghani et al. [19] have welded St52 steel to 5186 Al with threaded and unthreaded tool pin and showed that the best welds, presenting no tunnel defect and excellent strength, were performed with the threaded pin. Indeed, a thread causes extra material mixing due to an upwards/downwards material movement. Ramachandran et al. [21] also compared various tools with taper or straight cylindrical pins for welding 3-mm thick HSLA steel and 5052–H32 Al alloy. They found that a high taper angle of the pin (i.e. 20 or 30°) results in a less uniform interface and a need to enter more inside the steel plate in order to stir on the top and the bottom of the steel plate. Indeed, sufficient contact (typically a few tenth of millimetres) has to be made between the tool and the steel plate to ensure mixing and with an excessively tapered tool it is not the case at the bottom. However, a slight tapering (i.e. 10°) offered more beneficial stirring than the straight pin tool. Thus, as in similar FSW tunnel defect formation in dissimilar metal welds is limited by favouring material stirring through complex tool features like threading and tapering of the pin.

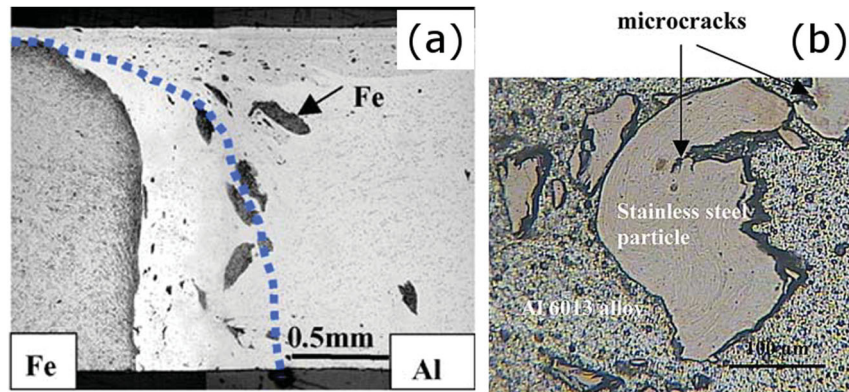


Figure 5. The presence of large pieces of steel inside the Al side of the nugget zone in Al–steel welds: (a) SS400 mild steel to 5082 Al alloy weld where the dotted blue line indicates the fracture path follows the steel pieces (from Watanabe et al. [52]); (b) X5CrNi18–10 stainless steel to Al 6013–T4 weld where micro-cracks are observed at the interface between the piece of stainless steel and the Al nugget (from Uzun et al. [51]).

The position of the softest material, i.e. on the AS or RS, also affects weld soundness. In Al to steel welds [17–21,40,52–54,56–58], Al to Ti welds [22–24,44], Mg to Ti welds [59] and Al to Cu welds [28,29,39,47], the softest material is placed on the RS in order to drag the hardest (steel, Ti or Cu) plate inside the softest (Al or Mg) plate. Galvao et al. [60] have also evidenced that in Al to Cu welds, this position of the Al plate may avoid the excessive flashes caused by the soft Al expulsion when placed on the AS (see Figure 6). The best position of the aluminium alloy to reach sound Al6061 to AZ31 welds is unclear [32,34,38] as Al and Mg have the same melting temperature and thus expectedly similar plasticisation temperatures. However, Firouzdor and Kou [32] and Dorbane et al. [38] suggest placing Al on the AS to avoid major tunnel defects. The placement of Al6061 on the AS and a large tool offset (tool mostly in Al side) leads to a higher torque, i.e. a higher heat input [32,34]. The resulting higher temperature [32] favours plasticisation (i.e. presents a lower flow stress) and thus avoids material flow-related defects.

Formation of intermetallic compounds

IMCs are generally formed at the interface between dissimilar metal welds with a good chemical affinity. Table 1 summarises the IMCs formed for many dissimilar metal butt and lap welds. These phases form in only a few seconds in solid state during FSW (see the section ‘Constitutional liquation in dissimilar welds’ for exceptions) and under large plastic deformation and may thus present an out-of-equilibrium formation [47]. Now, the issue is that they are generally brittle compounds [76]. The behaviour of the friction stir welds is a function of their nature, size, distribution and continuity/discontinuity.

In the *Al to steel* dissimilar welds, many studies report different IMCs, but it seems generally accepted that the stable and brittle Fe_2Al_5 phase is expected to form [17,19,40,61–63] in particular for low heat input

Table 1. Intermetallic compounds formed in dissimilar metal FSW.

Materials	Intermetallic observed	Ref.
Al to steel	Fe_2Al_5 , $\text{Fe}_4\text{Al}_{13}$	[61,62] (LpW)
	Fe_2Al_5 , FeAl_3	[16] (LpW)
	Fe_2Al_5 , FeAl_6	[19]
	FeAl (low rev min^{-1}) or FeAl_3 (high rev min^{-1})	[54]
	Fe_2Al_5 (low rev min^{-1}) or Fe_3Al , FeAl_2 (high rev min^{-1})	[40]
	Fe_2Al_5 , FeAl	[63] (LpW)
	FeAl_3	[20]
	FeAl , Fe_3Al	[41]
	$\text{Fe}_4\text{Al}_{13}$ (mainly), Fe_3Al	[64]
	Fe_2Al_5	[59]
Mg (+Al) to steel	Al_2Cu , Al_4Cu_9	[28,47,57,65–67]
	Al_2Cu , Al_4Cu_9 , AlCu	[26]
	Al_2Cu , Al_4Cu_9 , Al_2Cu_3	[68]
Al to Brass	Al_2Cu , Al_4Cu_9 , ZnCu	[46,69]
Al to Mg	$\text{Al}_{12}\text{Mg}_{17}$	[70]
	Al_3Mg_2 , $\text{Al}_{12}\text{Mg}_{17}$	[31,36]
Ti to steel	FeTi	[71] (LpW)
	FeTi , Fe_2Ti	[72,73] (LpW)
Al to Ti	TiAl_3	[74] (LpW) [24,44]
	TiAl_3	[75]

Notes: When available, the selected references preferentially identify the phases based on local probing characterisation techniques (e.g. transmission electron microscopy or X-ray diffraction). LpW, lap welding.

[40]. Das et al. [64] did not find much Fe_3Al intermetallic and associate that to the lack of diffusion time. Excess vacancies formation in the presence of large plastic deformation and strain rates may also modify the equilibrium phase formation [77,78]. This IMC was, however, observed in Al to steel FS welds by Ghosh et al. [40] for high rotational speed welds. The thickness of the various IMC layers (Table 1) increases as the heat input increases, i.e. the rotational speed increases [20,41,56,64], the advancing speed decreases [41,57,64] or if the pin is placed more inside the steel plate [41]. Lan et al. [41] show that the logarithm of the intermetallic layer thickness presents a linear decreasing dependence with the welding speed. The thickness of their IMC layer made of FeAl and Fe_3Al can be reduced to very small sizes (i.e. 150 nm) at the highest advancing speeds (i.e. 90 mm min^{-1}) and lowest rotational speed

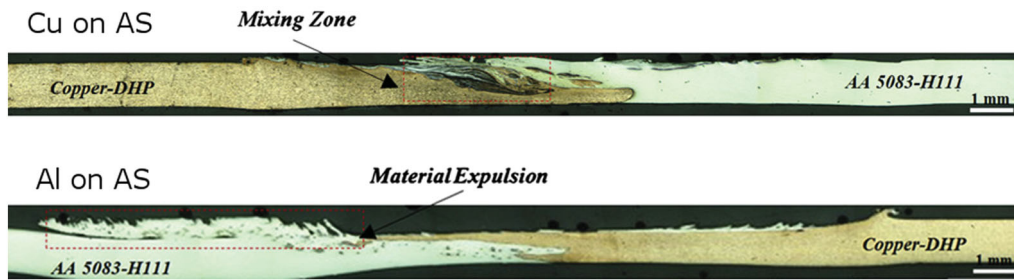


Figure 6. Comparison of Al 5083–H111 to Cu DHP welds with either (a) Cu placed on the AS or (b) Al placed on the AS. It evidences the formation of excessive flashes due to the soft Al expulsions when Al is placed on the AS (from Galvao et al. [60]).

(i.e. $1200 \text{ rev min}^{-1}$) with positive consequences on the strength at fracture (see the section ‘Joint mechanical properties’).

In the *Al to Cu* dissimilar welds, many IMC can form, but Al_2Cu and Al_4Cu_9 are systematically reported [26,28,46,47,57,65–69]. The ZnCu compound is also reported when welding *brass to Al* alloys [46,69]. Avettand-Fènoël et al. [47] have evidenced, by neutron diffraction pattern fitting, that the proportion of IMC is two times larger in welds when the tool is shifted towards the Al or Cu side. This is expected for the Cu offset welds as higher temperatures are reached. However, in the Al offset welds this is supposedly the results of more material mixing. A modified Al_2Cu IMC has also been found [47] and is associated with an out-of-equilibrium structure generated by intense plastic deformation and short-thermal cycles. An intercalated microstructure was also found in Al6082 to AlCu welds with bands rich in Al_4Cu_9 IMC [47]. The formation of this compound is favoured by its large volume expansion (23%) compared to Al_2Cu which relaxes the large residual stresses typical of dissimilar welding.

In the *Ti to steel* dissimilar welds, Fazel-Najafabadi et al. [71] report that FeTi is formed preferentially to Fe_2Ti because FeTi has a lower energy of formation at equilibrium. However, Fe_2Ti has been reported in Ti to steel dissimilar welds by Gao et al. [72] and Ishida [73] with a lower heat input, in particular a lower rotational speed [72,73] below 450 rev min^{-1} . Maybe its kinetic of formation is favoured by lattice defects expectedly formed during welding due to the large plastic deformation. This hypothesis could be verified using Monte Carlo kinetic modelling [79].

Welding *Al to Mg* generally leads to the $\text{Al}_{12}\text{Mg}_{17}$ compound [31,36,70]. In the *Mg to steel* as well as the *Mg to Ti* dissimilar welds, it is more the presence of Al in the magnesium alloy that is at the origin of the IMC, i.e. Fe_2Al_5 [59] and TiAl_3 , respectively [75]. TiAl_3 has also been reported when welding *Al to Ti* [24,44,74].

Joint mechanical properties

In this section, the joint strength will be exclusively discussed for butt welds. Indeed, these types of joints allow easy comparison with the strength of the base materials

contrarily to lap joints for which the shear configuration provides only a maximum force that is not easily converted into a tensile strength. Ogura et al. [80] present the only lap joint study, to the authors’ knowledge, that performs mini-tensile tests with the loading direction perpendicular to the interface for dissimilar lap joints. However, their joints had to be performed on thick plates (15 mm Al3003 to 12 mm 304 stainless steel) to be able to extract the mini-tensile samples. The thermal cycles near the interface are thus different to more classical thicknesses (typically 3 mm, see Table 2, column 2). They reach strength typically around 130 MPa in the weld centre, much below the strength that may be reached in butt welds (Table 2, column 7).

Al to steel dissimilar welds

Table 2 summarises the best tensile strength reached in reported papers as a function of the welding conditions of Al to steel dissimilar butt welds. Strengths in the range 200–333 MPa are reported if fracture occurs in the IMC layer (Table 2, column 7). The highest strength, i.e. 333 MPa, is associated with fracture in an extremely thin IMC layer, i.e. below 100 nm [56]. The best welding conditions cannot be generalised and expectedly depend on the nature of the base materials, in particular on their properties at the welding temperature. Optimum rotational speeds between 250 and $1800 \text{ rev min}^{-1}$ and advancing speeds between 23 and 480 mm min^{-1} have been reported (Table 2, columns 3 and 4). The highest advancing speed reached, i.e. 480 mm min^{-1} , is also associated with a high rotational speed, i.e. $1600 \text{ rev min}^{-1}$, to enhance heat input and expectedly favour material flow [17]. However, generally the optimum advancing speeds are rather low, i.e. below 100 mm min^{-1} (Table 2, column 3) for 12 cases out of the 15 reported in Table 2. The thickness of the plates is generally low: typically below or equal to 3 mm (Table 2, column 2), probably due to tool wear issues. The position of the tool in relation to the Al to steel interface seems to be best at a couple of 10th of mm to 1 mm of the steel interface (Table 2, columns 5 and 7). Indeed, as mentioned in the section ‘Material flow’, a larger tool offset inside the hardest plate favours the dispersion of a lot of steel pieces in the Al plate that may be

Table 2. Strength and welding parameters of the best friction stir butt welds of Al to steel.

Materials	T/mm	$v/\text{mm min}^{-1}$	$\omega/\text{rev min}^{-1}$	Offset	Position of Al	Strength/MPa	Ref.
Al1050–S235 steel	4	100	900	0	RS	80 (in Al BM)	[57]
Al1100–A441 steel	3	63	800	1.3	RS	80 (in Al BM)	[20]
Al5186–St52	3	56	355	0.2	RS	246	[19]
Al5083–mild steel	2	25	250	0.2	RS	237	[52]
Al5052–HSLA steel	3	45	500	0.2	RS	188	[21]
Al6181–DP600	1.5	480	1600	1.0	RS	211	[17]
Al6181–HSS	1.5	480	1600	1.0	RS	200	[17]
Al6016–mild steel	1.12	250	900	0.9	RS	210	[58]
Al6061–TRIP steel	1.5	90	1800	0.32	RS	240	[54]
Al6061–SS	6	54–72	550	0.1–0.2	RS	225–240	[53]
Al6061–304SS	3	30	710	< 0.1	RS	260	[40]
Al6061–304SS (FSW)	3	48	300	0.8	RS	244	[18]
Al6061–304SS (FSW + GTAW)	3	48	300	0.8	RS	290	[18]
Al6061–Q235 steel (FSW + LW)	3	23.5	950	0.8	RS	196	[43]
Al7075–mild steel	3	100	500	0.3–0	RS	333	[56]

Notes: If many welds are performed, the welding parameters providing the best strength are reported. T , plate thickness/mm; v , welding speed/mm min^{-1} ; ω , rotational speed/rev min^{-1} , offset is reported as the distance of insertion of the pin inside the steel plate; RS, retreating side, strength is the tensile strength at fracture/MPa; SS, stainless steel; HSS, high strength steel; GTAW, gas tungsten arc welding; LW, laser welding.

Table 3. Strength and welding parameters of the best friction stir butt welds of Mg to steel.

Materials	T/mm	$v/\text{mm min}^{-1}$	$\omega/\text{rev min}^{-1}$	Offset	Position of Al	Strength/MPa	Ref.
Pure Mg–low carbon steel						66	
AZ31–low carbon steel	2	100	1000	0.5	RS	170	[59]
AZ61–low carbon steel						220	

Notes: If many welds are performed, the welding parameters providing the best strength are reported. T , plate thickness (mm); v , welding speed/mm min^{-1} ; ω , rotational speed/rev min^{-1} , offset is reported as the distance of insertion of the pin inside the steel plate; AS, advancing side; RS, retreating side, strength is the tensile strength at fracture/MPa.

the preferential path for failure [17,51,52]. Tanaka et al. [56] suggest that the joint strength between Al and steel is inversely proportional to the heat input presented on a log scale [56]. This is directly associated with the thickness of the IMC layer (see the section ‘Formation of intermetallic compounds (IMC)’). Thus, to conclude, the heat input should be sufficient to ensure material mixing and avoid keeping a too sharp interface. Now, the heat input should also be limited to avoid excessive IMC layer growth. A good compromise has thus to be found.

Other mechanical properties than the tensile strength have also been reported. Uzun et al. [51] performed fatigue tests on Al6013 to stainless steel welds and found only 30% reduction in the fatigue life of the weld compared to the Al6013-T4 base material. The fatigue cracks initiated from the root side of the weld [51]. Chen [53,81] performed C-notched and V-notched Charpy impact tests on Al6061 to SS400 low carbon steel welds. At a rotational speed of 550 rev min^{-1} , the best absorbed energy is reached with a ductile fracture in the Al. At a rotational speed of 800 rev min^{-1} , a brittle fracture in the IMC was observed.

Mg to steel dissimilar welds

Table 3 shows that in the work by Kasai et al. [59] the strength of Mg to steel welds increases if the Al content of the Mg alloy is increasing. This is believed to be related to the Al depleted zone, where fracture occurs, that is formed at the vicinity of the IMC layer made of Fe_2Al_5 (Table 1). The higher Al content of the base alloys allows for that zone to be still made of sufficient

Al to retain some strengthening ability. No IMC layer is formed in the pure Mg to steel weld, due to a lack of reactivity, leading to low joint strength.

Al to Ti dissimilar welds

Table 4 summarises the best tensile strength reached in reported papers as a function of the welding conditions for Al to Ti dissimilar butt welds. The strength of the welds is in the 200–350 MPa range [22–24,44]. The rotational speeds are close to 1000 rev min^{-1} and relatively low welding speeds are used, i.e. 80–200 mm min^{-1} [22–24,44]. In the results of Song et al. [24], see also Figure 3, the strength of the welds was low if a sharp interface feature is observed or if the tool is too excessively inserted in the Ti plate which favours the formation of excessive IMC. Thus in-between tool offset should be selected, i.e. 0.6–0.9 mm.

Mg to Ti dissimilar welds

Table 5 summarises the best tensile strength reached in reported papers as a function of the welding conditions for Mg to Ti dissimilar butt welds. Aonuma et al. [45,75,82] mainly focussed on the effect of the alloying elements in Mg on the tensile strength of the welds. Strength from 150 to 250 MPa has been reached depending on the alloying element in Mg (Table 5, columns 1 and 7). In their 2009 article [82], they showed that increasing the Al content in the AZ alloys leads to significant strength reduction (Table 5) as more Al to Ti intermetallics (Table 1) are formed at the interface. In their 2010 article [75], they showed that increasing

Table 4. Strength and welding parameters of the best friction stir butt welds of Al to Ti.

Materials	T/mm	$v/\text{mm min}^{-1}$	$\omega/\text{rev min}^{-1}$	Offset	Position of Al	Strength/MPa	Ref.
Al6061–Ti6Al4V	2	200	750	1.2	RS	215	[44]
Al6061–Ti6Al4V	2	120	750–1000	0.6	RS	200	[24]
Al6Mg–Ti6Al4V	2	60	1200	0.5	RS	292	[23]
Al2024–Ti6Al4V	2	80	800	0.1	RS	348	[22]

Note: T , plate thickness/mm; v , welding speed/mm min^{-1} ; ω , rotational speed/rev min^{-1} , offset is reported as the distance of insertion of the pin inside the Ti plate; AS, advancing side; RS, retreating side, strength is the tensile strength at fracture/MPa.

Table 5. Strength and welding parameters of the best friction stir butt welds of Mg to Ti.

Materials	T/mm	$v/\text{mm min}^{-1}$	$\omega/\text{rev min}^{-1}$	Offset	Position of Al	Strength/MPa	Ref.
AZ31B–Ti						175	
AZ61A–Ti	2	50	850	0.5	AS	160	[82]
AZ91D–Ti						130	
AM60–Ti	2	1.5	AS	138	[75]
AM60 + 2%Ca–Ti						225	
Mg–Ti	2	50	850	1.5	RS	135	[45]
ZK60–Ti						237	

Note: T , plate thickness/mm; v , welding speed/mm min^{-1} ; ω , rotational speed/rev min^{-1} , offset is reported as the distance of insertion of the pin inside the Ti plate; AS, advancing side; RS, retreating side, strength is the tensile strength at fracture/MPa.

Table 6. Strength and welding parameters of the best friction stir butt welds of Al to Cu.

Materials	T/mm	$v/\text{mm min}^{-1}$	$\omega/\text{rev min}^{-1}$	Offset	Position of Al	Strength/MPa	Ref.
Al1050–brass (30% Zn)	1.5	8	450	0.7	RS	101	[46]
Al1060–pure Cu	5	100	600	1.0	RS	110	[29,65]
Al5A02–pure Cu	3	20	1100	1.3	AS	130	[68]
Al1060–pure Cu	3	100–200	600	1	...	130	[30]
Al6061–ETP Cu	6.3	40	1500	2.0	RS	133	[55]

Notes: If many welds are performed, the welding parameters providing the best strength are reported. T , plate thickness/mm; v , welding speed/mm min^{-1} ; ω , rotational speed/rev min^{-1} , offset is reported as the distance of insertion of the pin inside the Cu plate; AS, advancing side; RS, retreating side, strength is the tensile strength at fracture/MPa.

the Ca content in an AM60 alloy improves the strength from 138 to 225 MPa due to the formation of Al_2Ca compounds at the Mg to Ti interface in detriment to the TiAl_3 intermetallics (Table 1). In their 2012 article [45], they showed that the Zn and Zr alloying elements contained in the ZK60 alloy improved the joint strength from 135 MPa in a pure Mg alloy welded to Ti up to 237 MPa due to a reaction layer of Zn and Zr with Ti. Thus, the reaction layer has to be present to trigger welding, but a too thick one is undesirable as it favours earlier fracture.

Al to Cu dissimilar welds

Table 6 summarises the best tensile strength reached in reported papers as a function of the welding conditions for Al to Cu dissimilar butt welds. The strength of the welds is between 100 and 133 MPa (Table 6, column 7). Similarly to the Al to steel welds, there is no clear consensus as to what the best welding parameters are for optimal tensile strength; however, the advancing speeds for optimal strength remain low, i.e. $< 200 \text{ mm min}^{-1}$ (Table 6, column 3). The tool offset is slightly larger towards the Cu plate than in Al to steel welds, also because tool wear is not as much an issue in Al to Cu welds. Hard steel tools are often selected [26,28,47,55,68]. A larger tool offset favours a higher heat input and thus expectedly more plasticisation of Cu.

Al to Mg dissimilar welds

Table 7 summarises the best tensile strength reached in reported papers as a function of the welding conditions for Al to Mg dissimilar butt welds. There is a large scatter in the tensile strength of these various welds (82–250 MPa, Table 7, column 7). The lowest joint strengths are associated with the sharp interface features [33,35,37,49]. Venkateswaran et al. [33] found that the joint strength increases when the volume of the vortex-like zone increases. The position of the Al alloy in relation to the tool rotation has been varied in Al6061 to AZ31B welds leading to good tensile properties in both options when defects are avoided [32,34], see the section ‘Weld soundness and material mixing in butt welds’. Venkateswaran et al. [33] reported an increase of the joint strength when the IMC layer thickness was reduced from 4 to 2 μm , similarly to the work of Tanaka et al. [56] in Al to steel welds.

Constitutional liquation in dissimilar welds

Generally, melting is not observed in FSW and this is highly desirable as solid-state welding avoids solidification defects. Now, the temperature may reach the melting of a eutectic phase above the solidus temperatures of the base materials, i.e. constitutional liquation. Al to Mg dissimilar welds are particularly susceptible to this phenomenon [31,32,34,36,70,84,85]. Indeed, the

Table 7. Strength and welding parameters of the best friction stir butt welds of Al to Mg.

Materials	T/mm	$v/mm\ min^{-1}$	$\omega/rev\ min^{-1}$	Offset	Position of Al	Strength/MPa	Ref.
Al1060–AZ31	4	30	315	4 mm in Mg	AS	82	[31]
Al5052–AZ31B	3	200	1000	0	AS	147	[49]
Al5052–AZ31B	2	300	1000	0	AS	132	[35]
Al6061–AZ31B	1.6	250	1600	0	AS	250	[32]
Al6061–AZ31B	3	50	600–700	0.3 mm in Mg	RS	170	[34]
Al6061–AZ31B	3	500	1400		AS	168 (at 25°C) 86 (at 200°C)	[38]
Al6061–AZ31	6	20	400	0	RS	192	[83]
Al6063–AZ31B	3.25	117–202	900–1400	126	[33]
Al6013–AZ31 (underwater)	2.5	80	1200	0	AS	152	[50]
Al2924–AZ31B	5	50	300	0.7 mm in Mg	AS	107	[37]

Notes: If many welds are performed the welding parameters providing the best strength are reported. T , plate thickness/mm; v , welding speed/mm min^{-1} ; ω , rotational speed/rev min^{-1} , offset is reported as the distance of the tool centre from the butted interface; AS, advancing side; RS, retreating side, strength is the tensile strength at fracture/MPa.

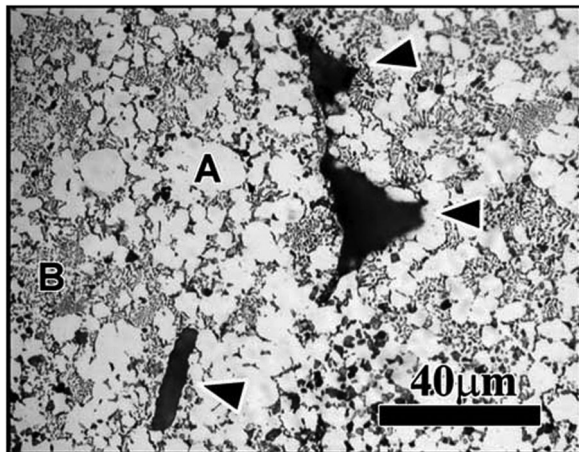


Figure 7. Evidence of eutectics resulting from constitutional liquation in a Al1050 to AZ31 weld performed at 1.5 mm min^{-1} and 2450 rev min^{-1} (from Sato et al. [70]).

Al to Mg phase diagram presents a deep eutectic at 450°C that leads to local melting. Such a temperature may indeed locally be reached in friction stir welds as the required homologous temperature for FSW is in-between 0.6 and 0.9 [2], i.e. it may reach 550°C for Al and Mg welds. Figure 7 presents the resulting eutectic microstructure in an Al1050 to AZ31 weld. This constitutional liquation may cause the formation of solidification cracks in the welds [31]. Firouzdor et al. [32] showed that constitutional liquation is the reason for excessive IMC in Al–Mg welds that are detrimental to their strength. Indeed, reactivity and diffusion in the liquid state are favoured and enhance the formation of IMC.

Table 8 summarises the welding conditions of reported literature mentioning constitutional liquation and the formation of a eutectic phase. Constitutional liquation may be avoided by lowering the weld heat input, i.e. with a lower rotational speed [31,32] or a higher advancing speed (comparing [31,32,35,36],

Table 8).¹ Firouzdor et al. [32] showed that the liquation phenomenon is only present in their welds for which Al was placed on the advancing side (AS). This again is consistent with a higher heat input, as they have measured a higher peak temperature in their dissimilar welds for which Al was placed on the AS.

Ouyang et al. [26] reported such a constitutional liquation in Al to Cu welds for which the eutectic temperature is at 548°C, below the 580°C they measured near the SZ. This leads to the growth of CuAl dendrites nucleating from the liquid phase. Galvao et al. [28] specifically reported that they do not observe eutectic structures in their welds with similar welding parameters. The main difference is the thickness of the plates, i.e. 12.7 [26] and 1 mm [28]. A thinner plate necessitates a smaller tool, and the weld is cooled by the backing plate causing lower maximum temperatures.

Particularities related to lap welding

Changing the joint configuration is a possible solution to weld thin to thick plates or to avoid placing a large part of the tool in the hard material. In lap welding (Figure 1(b)), the tool shoulder is not in contact with the hard material if the hard material is placed as bottom plate. Note that we are here talking about the hardest material at the welding temperature. Thus, in Al to steel [16,61–63,80,89,90], Al to Ti [74,91] and Mg to steel [92,93] dissimilar lap welds, Al or Mg is always placed on top of the steel or Ti plate in order for the tool to travel inside the softest material and limit its wear. Ti to steel welds have mainly been performed in lap joint configuration, and the Ti plate is generally placed on top [71–73,94,95] except in Fazel-Najafabadi et al. [71] where stainless steel is welded on top of Cp–Ti. Brass to steel welds have been little studied, but Gao et al. [96] have also placed the softest material, i.e. brass, on top. In Al to Cu dissimilar lap welds, Al is placed as top

¹ Firouzdor et al. [32] measured the temperature at 3 mm from the weldline for Al6061 to AZ31B welds when increasing the rotational speed from 1400 to 2200 rev min^{-1} for an advancing speed of 38 mm min^{-1} . They found typically a 45°C increase in temperature. When increasing the advancing speed from 38 to 254 mm min^{-1} at 1400 rev min^{-1} , the decrease in temperature was between 15 and 50°C.

Table 8. Comparison of the Al–Mg welds for the observation of constitutional liquation (C.L.).

Materials	T/mm	Diameter shoulder/pin/mm	v/mm min ⁻¹	ω /rev min ⁻¹	Offset	Position of Al or LpW	C.L. observed	Ref.
Al1050–AZ31	6	...	1.5	2450	0	RS	Yes	[70]
Al1060–AZ31	4	20/6	30	200–1000	0	AS	Yes	[31]
				1000	4 mm in Mg		Yes	
				200–800	4 mm in Mg		No	
Al5052–AZ31B	2	10/4	300	800–1400	0	AS	No	[35]
Al6040–AZ31	1.5	...	225	1400	0	RS	No	[36]
Al6061–AZ31B	1.6	10/4	38	2200	0	AS	Yes	[32]
			38, 254	1400		AS	No	
			38	2200		RS	No	
Al6061–AZ31B	3	10/3.2	50	700	0.3 mm in Mg	RS	Yes	[34]
<i>Lap welding</i>								
AC4C (top)–AZ31	3/2.5	15/5	20, 50, 80	1500	NR	LpW	Yes	[84]
Al6061–AZ31B (top)	2.3/3.1	18/5–6	25	1120	NR	LpW	Yes	[86]
			25	900			Yes	
			20	700			Yes	
			40	1400			Limited	
Al6022 (top)–AM60B	3.1/3.1	12/5.4	75	1500	NR	AS	Yes	[87]
<i>Underwater cooled</i>								
Al5083–AZ31C	3	20/7	50	300	0	AS	No	[88]
Al6013–AZ31	2.5	16/5	80	1200	0	AS	No	[50]

Notes: Only the welding parameters and papers that clearly showed evidences of C.L. as mentioned by the paper's authors are reported here. LpW, lap welding; NR, not relevant.

[66,69,97] or bottom plate [67,97,98]. Akbari et al. [98] compare the placement of Cu vs. Al on top. They conclude that placing the Al sheet on top is preferable as the lower thermal conductivity of Al generates more heat in the weld area, particularly under the shoulder, leading to less defected welds compared to placing the Cu sheet on top. This latter configuration leads to channel defects due to insufficient plastic flow and thus to lower lap shear strength. The IMC layer formed in both configurations is rather similar due to similar cooling rates for given rotational and advancing speeds [98]. In Al to Mg dissimilar welds, the plate that should be on top is unclear, similarly to the butt welds for which the best side for Al (AS or RS) is unclear. Al is on top in Chen and Nakata [84] and Rao et al. [87] and Mg is on top in Refs. [85,86]. The best lap shear strength for 20 mm wide samples is found to be 6.5 kN in Mohammadi et al. [85,86] compared to 3.6 kN in Chen and Nakata [84] and 2.2 kN in Rao et al. [87]. However, no systematic comparison with similar conditions in terms of material and tooling has been reported. Now, the choice should not affect tool wear.

Often the tool pin preferentially penetrates slightly in the bottom plate to ensure mechanical strength (Figure 1(b)). Of course, the tool wears out more if it is in contact with the hard plate, e.g. the steel plate in Al to steel welds. In Al to steel lap welds, the tool should slightly penetrate inside the steel to reach higher joint strength [61,99]. The tool penetration inside the steel plate leads to steel hook pushed upwards inside the upper Al plate on both sides of the tool, contrarily to the case where the tool does not penetrate the steel plate,

see Figure 8 for a stainless steel to Al1100 weld [99]. Such hook favours a mechanical anchorage (interlocking effect) increasing the joint strength [99]. Rao et al. [87] have also reported improvements of the lap shear strength of 6022-T4 to AM60B welds when a hook is formed. However, Jana et al. [93] have reported that in Mg to HSLA steel lap welds, the fatigue resistance of the weld is much lower than for similar Mg lap weld. They attribute this difference to the hooking effect of the steel in the Mg which acts as stress concentrators. Rao et al. [100] tested the fatigue properties of Al6022-T4 to AM60B lap welds and conclude that, at high applied stresses, the fracture is mainly dictated by the IMC and thus occurs at the Al to Mg interface. At lower stress levels, failure may occur in the Mg or the Al, usually near the hook. As expected, welds that presented defects like micro-voids in the SZ failed at the location of these defects. Thus, favouring hook formation improves the static strength, but it is the prime source of failure under fatigue loading.

The coating of the bottom material to enhance reactivity by melting at the interface and avoid the need for the penetration of the pin inside the bottom plate has also been considered [63,92,101], e.g. a Zn coating on the steel in an Al [63] or Mg [92,101] to high strength steel weld. Thus, a simple tool steel can be used [63]. In magnesium AZ31B to mild steel lap welds, Schneider et al. [92] report that the strength of the weld also increases if the steel has a 15- μ m thick Zn coating. This is attributed to the low melting point Mg–Zn eutectic melting during the process. The liquid fills pores and cracks that are detrimental to the weld strength in the

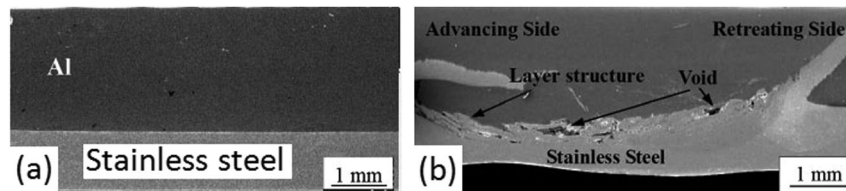


Figure 8. Al 1100 to stainless steel lap weld with (a) a short pin that does not penetrate in the weld joint and (b) with a longer pin that penetrates in the stainless steel plate, leading to the formation of a hook and some voids in the presence of a turbulent flow (from Xiong et al. [99]).

absence of the Zn coating. However, in that study, the pin did well plunge by 0.15 mm inside the steel plate. Finally, Akbari et al. [102] anodised an intermediate Cu layer on the top Al plate in an Al to Cu FS weld. The anodised layer presents a higher Cu content, preventing the formation of an IMC layer and thus enhancing the lap shear strength of the weld by 25%.

Process modifications

Heat input modifications

Some researchers have proposed to assist FSW with other welding processes to pre-heat the hardest plate, e.g. the steel plate in Al to steel welds [18,43] or the Cu plate in Al to Cu welds [103]. Bang et al. [18] performed gas tungsten arc assisted FSW of 6061 Al to 304 stainless steel. This preheating of the joint improved its ductility (from about 1 to 3%) as it led to a less brittle fracture. Indeed, the hybrid weld presented less welding defects and no steel parts were detected in the aluminium plate. Fei et al. [43] performed laser-assisted FSW in order to soften the steel plate and favour material flow in the steel plate. Yaduwanshi et al. [103] showed, by their thermal model of plasma-assisted dissimilar Al to Cu FSW, that the highest temperatures are moved towards the Cu side by the plasma assistance. This corresponds to 10 MPa decrease in yield strength of the Cu and hence favour Cu material mixing with Al. Now, increasing the heat input will expectedly favour the formation of a thicker IMC layer which is not leading to the best mechanical properties [56]. It seems thus that, in the studies mentioned here [18,43,103], it is the enhanced material mixing which is at the origin of the improvement in mechanical properties. Liu et al. [104] have proposed to perform electrically assisted FSW of 6061 Al alloy to TRIP steel. They found that the axial force is reduced and that the plunge stage is facilitated due to Joule effect as well as electro-plastic effect, i.e. the facilitation of the dislocation movements due to electron migration. However, the electrical current also promotes the formation of the IMC due to enhanced diffusion.

Now decreasing the heat input is more desirable in other dissimilar welding material couples, in order to limit the formation of IMC. Underwater welding is a way to cool the structure and avoid IMC growth.

Underwater welding has been attempted by Zhang et al. [67] for an Al6061 to Cu dissimilar weld. The peak temperature was decreased by 29°C, and the hot working time decreased. The IMC layer thickness decreased from 18 to 2 µm due to a disappearance of constitutional liquation. Underwater welding was also performed for Al to Mg welds and a much thinner [50] or no [88] IMC layer was evidenced (Table 8). Zhao et al. [50] have shown that underwater cooling during welding is an option to weld with low advancing speed (80 mm min⁻¹) and medium rotational speed (1200 rev min⁻¹) and still avoid constitutional liquation.

External mean of modifying the IMC distribution

Strass et al. [105] have used ultrasounds to assist FSW. They managed to more homogeneously distribute the IMC and thus avoid the localisation of fracture near a thick uniform layer. A vortex-like flow is also favoured at the expense of the sharp interface. Their preliminary results show a 30% increase in strength in an Al5454 to AZ91 magnesium alloy weld.

Modification of the workpiece geometry

Ogura et al. [89] grooved the lower steel plate in an Al to steel lap weld in order to enhance the flow of aluminium inside the steel plate and make use of mechanical interlocking to improve the shear strength of the joint.

Process involving interface melting

In the section ‘Particularities related to lap welding’, the option of a local melting at the interface to enhance reactivity has already been discussed. Now this has not only been exploited for coated base plates. Indeed, Zhang et al. [106] performed a process that they called friction stir brasing to weld Al to steel in a lap joint configuration by melting a thin Zn layer at the Al to steel interface. The process is performed without a tool pin and leads to excellent mechanical properties of the joint. Kuang et al. [107] also applied this strategy to lap weld Al to Cu, inserting a 0.2-mm thick Zn foil in between the two plates. The IMC layer thickness can reach up to 100 µm and still reach good failure loads, while this IMC sounds very thick. Van der Rest et al. [108] and Crucifix et al. [109] also performed Al to steel

welds with the process they called friction melt bonding. In that process, the steel plate is placed on top of the Al plate and the pinless WC tool generates enough heat to melt the Al plate and generate an IMC sealing the joint. The mechanical properties of these welds are similar to what can be reached by classical dissimilar FSW. In all these modified processes, the welding tool is reduced to a simple cylinder facilitating tool manufacturing. Now these processes cannot be strictly classified as solid-state processes as here melting of one of the two materials to be joined is reached.

The friction stir scribe technology

Friction stir scribe (FSS) uses a pin tool ending with a tungsten carbide scribe insert that is used to perform lap welding [99,110–112]. The scribe, presenting good wear resistance, is the only part of the tool that penetrates inside the harder bottom plate and locally forges it. This technology allows to use tools made of hard steel and still favour good mixing at the interface favouring the formation of a hook (similarly to the hook in Figure 8(b)) [99,110,112].

General trends in dissimilar metal welding

Some general trends in dissimilar metal welding can be deduced from the paper discussions. In what concerns the IMC, it can be concluded that

- (i) The strength of dissimilar metal welds is mainly dictated by the IMC nature and distribution and thus similar metal combinations lead to similar strength except in the Al to Mg dissimilar weld combination where the scatter in reached strength is much larger. The thickness of the IMC layer should, however, be limited to enhance the mechanical performances. Generally IMC layer thickness in the 1- μm size range or slightly below is desirable. This IMC layer thickness increases with increasing heat input. Fine intermetallics also favour a better toughness.
- (ii) The addition of extra alloying elements leading to IMC may significantly improve the weld's strength. The suppression of this metallurgical reaction leads to bad joint strength.
- (iii) Constitutional liquation may be observed in Al to Mg and sometimes even in Al to Cu dissimilar welds enhancing the formation of IMC due to higher reactivity in the liquid state. Welding with low heat input or underwater welding is a way to reduce constitutional liquation.
- (iv) The formation of brittle IMC is certainly a major break in the general development of dissimilar metal welding. The mastering of the IMC in dissimilar welds and ways of avoiding their formation have not been sufficiently undertaken.

Current studies are more devoted to analysing their formation and distribution.

In what concerns material flow, the geometrical position of the different metals and in general the welding parameters, it can be concluded that

- (i) The difference in plasticisation temperatures of the different metals welded together affects significantly the material flow and may lead to defects specific to dissimilar metal welding, in particular tunnel defects and cracks in the IMC layers.
- (ii) Vortex-like flow is usually observed in high heat input welds and when offsetting the tool more in the hardest material. A sharp interface is generally observed at lower heat input.
- (iii) The softest material should be placed on the retreating side in butt welds to drag the hard material inside the soft material.
- (iv) In lap welds, the lowest strength material should be placed on top to limit tool wear. The tool should, however, penetrate slightly in the bottom plate to form a hook that enhances strength, but may also be a source of stress concentration and fatigue loading.
- (v) In metal combinations that present less differences in melting temperature (e.g. Al to Mg) the best position of the base materials in butt or lap welds is not so clear.
- (iv) When welding a low with a high melting point material (e.g. Al to steel, Al to Ti, Mg to Ti and to some extent Al to Cu), the offset distance should be kept minimal (i.e. most of the tool pin should remain inside the soft material) to enable a suitable plasticisation of the hard material, to limit tool wear and avoid the excessive insertion of fine hard particles inside the soft material that might be a preferential path for the crack propagation.
- (v) The welding speeds leading to the highest strength are rather low, i.e. 50–250 mm min^{-1} classically with some limited exceptions. Thus the productivity is not so high for dissimilar metal friction stir welds. The exact best parameter is, however, not clear for a given material combination and requires further investigation to understand what causes optimal parameters to be selected in a specific case.

Many modifications to the classical FSW process have been proposed in order to

- (i) favour mixing, e.g. by increasing the heat input in the high-temperature material or using the friction stir scribe technology or by changing the joint geometry;
- (ii) exploit the difference in melting point and favour reactivity by local melting either of a coating, of an

- added layer or even of the low melting point base material;
- (iii) modify the intermetallic layer, e.g. by added ultrasounds.

Acknowledgements

A. Simar acknowledges the financial support of the IAP Program from the Belgian State through the Belgian Policy Agency, contract IAP7/21 'INTEMATE'. The authors have interacted as part of the SF2M-AFM commission on FSW. N. Jimenez-Mena is thanked for making Figure 1.

Disclosure statement

No potential conflict of interest was reported by the authors.

References

- [1] Thomas WM, Nicholas ED, Needham JC, et al. Improvements to friction welding. UK patent application no. 9125978.8. US Patent 5460317; 1995.
- [2] Mishra RS, Ma ZY. Friction stir welding and processing. *Mater Sci Eng R*. 2005;50:1–78.
- [3] Mishra RS, De PS, Kumar N. Friction stir welding and processing: science and engineering. New York (NY): Springer; 2014.
- [4] Nandan R, DebRoy T, Bhadeshia HKDH. Recent advances in friction stir welding – process, weldment structure and properties. *Progress Mater Sci*. 2008;53:980–1023.
- [5] Threadgill PL, Leonard AJ, Shercliff HR, et al. Friction stir welding of aluminium alloys. *Int Mater Rev*. 2009;54:49–93.
- [6] Avettand-Fènoël M-N, Simar A. A review about friction stir welding of metal matrix composites. *Mater Charact*. 2016;120:1–17.
- [7] Eslami S, Tavares PJ, Moreira PMGP. Friction stir welding tooling for polymers: review and prospects. *Int J Adv Manuf Technol*. 2016;1–14.
- [8] Shtrikman MS. Current state and development of friction stir welding (review): Part 2: improvement of tools and welding method. *Weld Int*. 2008;22:712–719.
- [9] Rai R, De A, Bhadeshia HKDH, et al. Review, friction stir welding tools. *Sci Technol Weld Join*. 2011;16:325–342.
- [10] Yang XW, Fu T, Li WY. Friction stir spot welding: a review on joint macro and microstructure, property, and process modelling. *Adv Mater Sci Eng*. 2014;697170.
- [11] Somasekharan AC, Murr LE. Microstructures in friction-stir welded dissimilar magnesium alloys and magnesium alloys to 6061-T6 aluminum alloy. *Mater Charact*. 2004;52:49–64.
- [12] Murr LE. A review of FSW research on dissimilar metal and alloy systems. *J Mater Eng Perform*. 2010;19:1071–1089.
- [13] Jonckheere C, de Meester B, Denquin A, et al. Torque, temperature and hardening precipitation evolution in dissimilar friction stir welds between 6061-T6 and 2014-T6 aluminum alloys. *J Mater Process Technol*. 2013;213:826–837.
- [14] DebRoy T, Bhadeshia HKDH. Friction stir welding of dissimilar alloys – a perspective. *Sci Technol Weld Join*. 2010;15(4):266–270.
- [15] Ikuta A, Yin YH, North TH. Influence of tool thread on mechanical properties of dissimilar Al alloy friction stir spot welds. *Sci Technol Weld Join*. 2012;8:622–629.
- [16] Coelho RS, Kostka A, Sheikhi S, et al. Microstructure and mechanical properties of an AA6181-T4 aluminium alloy to HC340LA high strength steel friction stir overlapweld. *Adv Eng Mater*. 2008;10:961–972.
- [17] Coelho RS, Kostka A, dos Santos JF, et al. Friction-stir dissimilar welding of aluminium alloy to high strength steels: mechanical properties and their relation to microstructure. *Mater Sci Eng A*. 2012;556:175–183.
- [18] Bang HS, Jeon GH, Oh IH, et al. Gas tungsten arc welding assisted hybrid friction stir welding of dissimilar materials Al6061-T6 aluminum alloy and STS304 stainless steel. *Mater Des*. 2012;37:48–55.
- [19] Dehghani M, Amadeh A, Akbari Mousavi SAA. Investigations on the effects of friction stir welding parameters on intermetallic and defect formation in joining aluminum alloy to mild steel. *Mater Des*. 2013;49:433–441.
- [20] Derazkola HA, Aval HJ, Elyasi M. Analysis of process parameters effects on dissimilar friction stir welding of AA1100 and A441 AISI steel. *Sci Technol Weld Join*. 2015;20(7):553–562.
- [21] Ramachandran KK, Murugan N, Shashi Kumar S. Effect of tool axis offset and geometry of tool pin profile on the characteristics of friction stir welded dissimilar joints of aluminium alloy AA5052 and HSLA steel. *Mater Sci Eng A*. 2015;639:219–233.
- [22] Dressler U, Biallas G, Mercado UA. Friction stir welding of titanium alloy TiAl6V4 to aluminium alloy AA2024-T3. *Mater Sci Eng A*. 2009;526:113–117.
- [23] Li B, Zhang Z, Shen Y, et al. Dissimilar friction stir welding of Ti–6Al–4V alloy and aluminum alloy employing a modified butt joint configuration: Influences of process variables on the weld interfaces and tensile properties. *Mater Des*. 2014;53:838–848.
- [24] Song Z, Nakata K, Wu A, et al. Influence of probe offset distance on interfacial microstructure and mechanical properties of friction stir butt welded joint of Ti6Al4V and A6061 dissimilar alloys. *Mater Des*. 2014;57:269–278.
- [25] Murr LE, Li Y, Flores RD, et al. Intercalation vortices and related microstructural features in the friction-stir welding of dissimilar metals. *Mater Res Innovat*. 1998;2:150–163.
- [26] Ouyang J, Yarrapareddy E, Kovacevic R. Microstructural evolution in the friction stir welded 6061 aluminum alloy (T6-temper condition) to copper. *J Mater Process Technol*. 2006;172:110–122.
- [27] Liu P, Shi Q, Wang W, et al. Microstructure and XRD analysis of FSW joints for copper T2/aluminium 5A06 dissimilar materials. *Mater Lett*. 2008;62:4106–4108.
- [28] Galvao I, Oliveira JC, Loureiro A, et al. Formation and distribution of brittle structures in friction stir welding of aluminium and copper: influence of process parameters. *Sci Technol Weld Join*. 2011;16:681–689.
- [29] Xue P, Ni DR, Wang D, et al. Effect of friction stir welding parameters on the microstructure and mechanical properties of the dissimilar Al–Cu joints. *Mater Sci Eng A*. 2011;528:4683–4689.
- [30] Xue P, Xiao B, Ma Z. Microstructure and mechanical properties of friction stir welded dissimilar Al–Cu thin plate joints. *Proc. 10th Int. Sympo. FSW, Beijing, China; 2014.*

- [31] Yan J, Xu Z, Li Z, et al. Microstructure characteristics and performance of dissimilar welds between magnesium alloy and aluminum formed by friction stirring. *Scr Mater.* 2005;53:585–589.
- [32] Firouzdor V, Kou S. Al-to-Mg friction stir welding: effect of material position, travel speed and rotation speed. *Metall Mater Trans A.* 2010;41:2914–2935.
- [33] Venkateswaran P, Reynolds AP. Factors affecting the properties of friction stir welds between aluminum and magnesium alloys. *Mater Sci Eng A.* 2012;545:26–37.
- [34] Fu B, Qin G, Li F, et al. Friction stir welding process of dissimilar metals of 6061-T6aluminum alloy to AZ31B magnesium alloy. *J Mater Process Technol.* 2015;218:38–47.
- [35] Kwon YJ, Shigematsu I, Saito N. Dissimilar friction stir welding between magnesium and aluminum alloys. *Mater Lett.* 2008;62:3827–3829.
- [36] Kostka A, Coelho RS, dos Santos J, et al. Microstructure of friction stir welding of aluminium alloy to magnesium alloy. *Scr Mater.* 2009;60:953–956.
- [37] Jagadeesha CB. Dissimilar friction stir welding between aluminum alloy and magnesium alloy at a low rotational speed. *Mater Sci Eng A.* 2014;616:55–62.
- [38] Dorbane A, Mansoor B, Ayoub G, et al. Mechanical, microstructural and fracture properties of dissimilar welds produced by friction stir welding of AZ31B and Al6061. *Mater Sci Eng A.* 2016;651:720–733.
- [39] Galvao I, Leal RM, Loureiro A, et al. Material flow in heterogeneous friction stir welding of aluminium and copper thin sheets. *Sci Technol Weld Join.* 2010;15(8):654–660.
- [40] Ghosh M, Gupta RK, Hussain MM. Friction stir welding of stainless steel to Al alloy: effect of thermal condition on weld nugget microstructure. *Metall Mater Trans A.* 2014;45:854–863.
- [41] Lan S, Liu X, Ni J. Microstructural evolution during friction stir welding of dissimilar aluminum alloy to advanced high-strength steel. *Int J Adv Manuf Technol.* 2016;82(9):2183–2193.
- [42] Tanaka T, Hirata T, Shinomiya N, et al. Analysis of material flow in the sheet forming of friction-stir welds on alloys of mild steel and aluminum. *J Mater Process Technol.* 2015;226:115–124.
- [43] Fei X, Jin X, Ying Y, et al. Effect of pre-hole offset on the property of the joint during laser assisted friction stir welding of dissimilar metals steel and aluminium alloys. *Mater Sci Eng A.* 2016;653:43–52.
- [44] Wu A, Song Z, Nakata K, et al. Interface and properties of the friction stir welded joints of titanium alloy Ti6Al4V with aluminum alloy 6061. *Mater Des.* 2015;71:85–92.
- [45] Aonuma M, Nakata K. Dissimilar metal joining of ZK60 magnesium alloy and titanium by friction stir welding. *Mater Sci Eng B.* 2012;177:543–548.
- [46] Esmaeili A, Besharati Givi MK, Zareie Rajani HR. A metallurgical and mechanical study on dissimilar friction stir welding of aluminum 1050 to brass (CuZn30). *Mater Sci Eng A.* 2011;528:7093–7102.
- [47] Avettand-Fénoël MN, Taillard R, Ji G, et al. Multiscale study of interfacial intermetallic compounds in a dissimilar Al 6082-T6/Cu friction-stir weld. *Metall Mater Trans A.* 2012;43:4655–4666.
- [48] Safi SV, Amirabadi H, Givi MKB, et al. The effect of preheating on mechanical properties of friction stir welded dissimilar joints of copper and AA7075 aluminium alloy sheets. *Int J Adv Manuf Technol.* 2016;84(9):2401–2411.
- [49] Morishige T, Kawaguchi A, Tsujikawa M, et al. Dissimilar welding of Al and Mg alloys by FSW. *Mater Trans.* 2008;49:1129–1131.
- [50] Zhao Y, Lu Z, Yan K, et al. Microstructural characterizations and mechanical properties in underwater friction stir welding of aluminium and magnesium dissimilar alloys. *Mater Des.* 2015;65:675–681.
- [51] Uzun H, DalleDonne C, Argagnotto A, et al. Friction stir welding of dissimilar Al 6013-T4 to X5CrNi18-10 stainless steel. *Mater Des.* 2005;26:41–46.
- [52] Watanabe T, Takayama H, Yanagisawa A. Joining of aluminum alloy to steel by friction stir welding. *J Mater Process Technol.* 2006;178:342–349.
- [53] Chen T. Process parameters study on FSW joint of dissimilar metals for aluminum–steel. *J Mater Sci.* 2009;44:2573–2580.
- [54] Liu X, Lan S, Ni J. Analysis of process parameters effects on friction stir welding of dissimilar aluminum alloy to advanced high strength steel. *Mater Des.* 2014;59:50–62.
- [55] Mehta KP, Badheka VJ. Influence of tool design and process parameters on dissimilar friction stir welding of copper to AA6061-T651 joints. *Int J Adv Manuf Technol.* 2015;80(9):2073–2082.
- [56] Tanaka T, Morishige T, Hirata T. Comprehensive analysis of joint strength for dissimilar friction stir welds of mild steel to aluminum alloys. *Scr Mater.* 2009;61:756–759.
- [57] Girard M, Huneau B, Genevois C, et al. Friction stir diffusion bonding of dissimilar metals. *Sci Technol Weld Join.* 2010;15:661–665.
- [58] Mertin C, Naumov A, Mosecker L, et al. Influence of the process temperature on the properties of friction stir welded blanks made of mild steel and aluminium. *Key Eng Mater.* 2014;611–612:1429–1436.
- [59] Kasai H, Morisada Y, Fujii H. Dissimilar FSW of immiscible materials: steel/magnesium. *Mater Sci Eng A.* 2015;624:250–255.
- [60] Galvao I, Leitão C, Loureiro A, et al. Study of the welding conditions during similar and dissimilar aluminium and copper welding based on torque sensitivity analysis. *Mater Des.* 2012;42:259–264.
- [61] Elrefaey A, Takahashi M, Ikeuchi K. Friction-stir-welded lap joint of aluminum to zinc-coated steel. *J Japan Weld Soc.* 2005;23:186–193.
- [62] Chen YC, Nakata K. Effect of the surface state of steel on the microstructure and mechanical properties of dissimilar metal lap joints of aluminium and steel by friction stir welding. *Metall Mater Trans A.* 2008;39:1985–1992.
- [63] Haghshenas M, Abdel-Gwad A, Omran AM, et al. Friction stir weld assisted diffusion bonding of 5754 aluminum alloy to coated high strength steels. *Mater Des.* 2014;55:442–449.
- [64] Das H, Jana SS, Pal TK, et al. Numerical and experimental investigation on friction stir lap welding of aluminium to steel. *Sci Technol Weld Join.* 2014;19(1):69–75.
- [65] Xue P, Xiao BL, Ni DR, et al. Enhanced mechanical properties of friction stir welded dissimilar Al–Cu joint by intermetallic compounds. *Mater Sci Eng A.* 2010;527:5723–5727.
- [66] Xue P, Xiao BL, Ni DR, et al. Achieving high property friction stir welded aluminium/copper lap joint at low heat input. *Sci Technol Weld Join.* 2011;16:657–661.

- [67] Zhang J, Shen Y, Yao X, et al. Investigation on dissimilar underwater friction stir lap welding of 6061-T6 aluminum alloy to pure copper. *Mater Des.* **2014**;64:74–80.
- [68] Tan CW, Jiang ZG, Li LQ, et al. Microstructural evolution and mechanical properties of dissimilar Al–Cu joints produced by friction stir welding. *Mater Des.* **2013**;51:466–473.
- [69] Akbari M, Behnagh RA. Dissimilar friction-stir lap joining of 5083 aluminum alloy to CuZn34 brass. *Metall Mater Trans B.* **2012**;43:1177–1186.
- [70] Sato YS, Park SHC, Michiuchi M, et al. Constitutional liquation during dissimilar friction stir welding of Al and Mg alloys. *Scr Mater.* **2004**;50:1233–1236.
- [71] Fazel-Najafabadi M, Kashani-Bozorg SF, Zarei-Hanzaki A. Joining of CP-Ti to 304 stainless steel using friction stir welding technique. *Mater Des.* **2010**;31:4800–4807.
- [72] Gao Y, Nakata K, Nagatsuka K, et al. Interface microstructural control by probe length adjustment in friction stir welding of titanium and steel lap joint. *Mater Des.* **2015**;65:17–23.
- [73] Ishida K, Gao Y, Nagatsuka K, et al. Microstructures and mechanical properties of friction stir welded lap joints of commercially pure titanium and 304 stainless steel. *J Alloys Compounds.* **2015**;630:172–177.
- [74] Chen YC, Nakata K. Microstructural characterization and mechanical properties in friction stir welding of aluminum and titanium dissimilar alloys. *Mater Des.* **2009**;30:469–474.
- [75] Aonuma M, Nakata K. Effect of calcium on intermetallic compound layer at interface of calcium added magnesium–aluminum alloy and titanium joint by friction stir welding. *Mater Sci Eng B.* **2010**;173:135–138.
- [76] Kimura Y, Pope DP. Ductility and toughness in intermetallics. *Intermetallics.* **1998**;6:567–571.
- [77] Militzer M, Sun WP, Jonas JJ. Modelling the effect of deformation-induced vacancies on segregation and precipitation. *Acta Metall Mater.* **1994**;42:133–41.
- [78] Gunduz IE, Ando T, Shattuck E, et al. Enhanced diffusion and phase transformations during ultrasonic welding of zinc and aluminum. *Scr Mater.* **2005**;52:939–43.
- [79] Hin C, Brechet Y, Maugis P, et al. Kinetics of heterogeneous dislocation precipitation of NbC in alpha-iron. *Acta Mater.* **2008**;56:5535–5543.
- [80] Ogura T, Saito Y, Nishida T, et al. Partitioning evaluation of mechanical properties and the interfacial microstructure in a friction stir welded aluminum alloy/stainless steel lap joint. *Scr Mater.* **2012**;66:531–534.
- [81] Chen TP, Lin WB. Optimal FSW process parameters for interface and welded zone toughness of dissimilar aluminium–steel joint. *Sci Technol Weld Join.* **2010**;15(4):279–285.
- [82] Aonuma M, Nakata K. Effect of alloying elements on interface microstructure of Mg–Al–Zn magnesium alloys and titanium joint by friction stir welding. *Mater Sci Eng B.* **2009**;161:46–49.
- [83] Malarvizhi S, Balasubramanian V. Influences of tool shoulder diameter to plate thickness ratio (D/T) on stir zone formation and tensile properties of friction stir welded dissimilar joints of AA6061 aluminum–AZ31B magnesium alloys. *Mater Des.* **2012**;40:453–460.
- [84] Chen YC, Nakata K. Friction stir lap joining aluminum and magnesium alloys. *Scr Mater.* **2008**;58:433–436.
- [85] Mohammadi J, Behnamian Y, Mostafaei A, et al. Friction stir welding joint of dissimilar materials between AZ31B magnesium and 6061 aluminum alloys: microstructure studies and mechanical characterizations. *Mater Charact.* **2015**;101:189–207.
- [86] Mohammadi J, Behnamian Y, Mostafaei A, et al. Tool geometry, rotation and travel speeds effects on the properties of dissimilar magnesium/aluminum friction stir welded lap joints. *Mater Des.* **2015**;75:95–112.
- [87] Rao HM, Ghaffari B, Yuan W, et al. Effect of process parameters on microstructure and mechanical behaviors of friction stir linear welded aluminium to magnesium. *Mater Sci Eng A.* **2016**;651:27–36.
- [88] Mofid MA, Abdollah-Zadeh A, Malek Ghaini F. The effect of water cooling during dissimilar friction stir welding of Al alloy to Mg alloy. *Mater Des.* **2012**;36:161–167.
- [89] Ogura T, Nishida T, Tanaka Y, et al. Microscale evaluation of mechanical properties of friction stir welded A6061 aluminium alloy/304 stainless steel dissimilar lap joint. *Sci Technol Weld Join.* **2013**;18:108–113.
- [90] Nishida T, Ogura T, Nishida H, et al. Formation of interfacial microstructure in a friction stir welded lap joint between aluminium alloy and stainless steel. *Sci Technol Weld Join.* **2014**;19(7):609–616.
- [91] Chen ZW, Yazdani S. Microstructures in interface region and mechanical behaviours of friction stir lap Al6060 to Ti-6Al-4V welds. *Mater Sci Eng A.* **2015**;634:37–45.
- [92] Schneider C, Weinberger T, Inoue J, et al. Characterisation of interface of steel/magnesium FSW. *Sci Technol Weld Join.* **2011**;16:100–106.
- [93] Jana S, Hovanski Y. Fatigue behaviour of magnesium to steel dissimilar friction stir lap joints. *Sci Technol Weld Join.* **2012**;17:141–145.
- [94] Campo KN, Campanelli LC, Bergmann L, et al. Microstructure and interface characterization of dissimilar friction stir welded lap joints between Ti-6Al-4V and AISI 304. *Mater Des.* **2014**;56:139–145.
- [95] Buffa G. Joining Ti6Al4V and AISI 304 through friction stir welding of lap joints: experimental and numerical analysis. *Int J Mater Form.* **2016**;9:59–70.
- [96] Gao Y, Nakata K, Nagatsuka K, et al. Optimizing tool diameter for friction stir welded brass/steel lap joint. *J Mater Process Technol.* **2016**;229:313–321.
- [97] Galvao I, Verdera D, Gesto D, et al. Influence of aluminium alloy type on dissimilar friction stir lap welding of aluminium to copper. *J Mater Process Technol.* **2013**;213:1920–1928.
- [98] Akbari M, Abdi Behnagh R, Dadvand A. Effect of materials position on friction stir lap welding of Al to Cu. *Sci Technol Weld Join.* **2012**;17(7):581–588.
- [99] Xiong JT, Li JL, Qian JW, et al. High strength lap joint of aluminium and stainless steels fabricated by friction stir welding with cutting pin. *Sci Technol Weld Join.* **2012**;17:196–201.
- [100] Rao HM, Jordon JB, Ghaffari B, et al. Fatigue and fracture of friction linear welded dissimilar aluminum-to-magnesium alloys. *Int J Fatigue.* **2016**;82:737–747.
- [101] Jana S, Hovanski Y, Grant GJ. Friction stir lap welding of magnesium alloy to steel: a preliminary investigation. *Metall Mater Trans A.* **2010**;41:3173–3182.
- [102] Akbari M, Bahemmat P, Haghpanahi M, et al. Enhancing metallurgical and mechanical properties of friction stir lap welding of Al–Cu using intermediate layer. *Sci Technol Weld Join.* **2013**;18:518–524.
- [103] Yaduwanshi DK, Bag S, Pal S. Numerical modeling and experimental investigation on plasma-assisted hybrid

- friction stir welding of dissimilar materials. *Mater Des.* **2016**;92:166–183.
- [104] Liu X, Lan S, Ni J. Electrically assisted friction stir welding for joining Al 6061 to TRIP780 steel. *J Mater Process Technol.* **2015**;219:112–123.
- [105] Strass B, Wagner G, Eifler D. Ultrasound supported friction stir welding of Al/Mg-hybrid-joint. Proceedings of 10th International Symposium on FSW, Beijing, China; 2014.
- [106] Zhang G, Su W, Zhang J, et al. Friction stir brazing: a novel process for fabricating Al/Steel layered composite and for dissimilar joining of Al to steel. *Metall Mater Trans A.* **2011**;42:2850–2861.
- [107] Kuang B, Shen Y, Chen W, et al. The dissimilar friction stir lap welding of 1A99 Al to pure Cu using Zn as filler metal with pinless tool configuration. *Mater Des.* **2015**;68:54–62.
- [108] van der Rest C, Jacques PJ, Simar A. On the joining of steel and aluminium by means of a new friction melt bonding process. *Scr Mater.* **2014**;77:25–28.
- [109] Crucifix S, van der Rest C, Jimenez-Mena N, et al. Modelling thermal cycles and intermetallic growth during friction melt bonding of ULC steel to aluminium alloy 2024-T3. *Sci Technol Weld Join.* **2015**;20:319–324.
- [110] Jana S, Hovanski Y, Grant GJ, et al. Effect of tool features on the joint strength of dissimilar friction stir lap welds. Friction Stir Welding and Processing VI, TMS Annual Meeting; 2011. p. 205–211.
- [111] Curtis T, Widener C, West M, et al. Friction stir scribe welding of dissimilar aluminum to steel lap joints. Friction Stir Welding and Processing VIII, TMS Annual Meeting; 2015. p. 163–169.
- [112] Patterson EE, Hovanski Y, Field DP. Microstructural characterization of friction stir welded aluminum-steel joints. *Metall Mater Trans A.* **2016**;47(6):2815–2829.